

Evidence of d -wave superconductivity in $K_{1-x}Na_xFe_2As_2$ ($x = 0, 0.1$) single crystals from low-temperature specific-heat measurements

M. Abdel-Hafiez,^{1,*} V. Grinenko,^{1,*} S. Aswartham,¹ I. Morozov,^{1,†} M. Roslova,^{1,†} O. Vakaliuk,¹ S. Johnston,^{1,‡} D. V. Efremov,¹ J. van den Brink,^{1,2} H. Rosner,³ M. Kumar,¹ C. Hess,¹ S. Wurmehl,¹ A. U. B. Wolter,¹ B. Büchner,^{1,4} E. L. Green,⁵ J. Wosnitza,^{4,5} P. Vogt,⁶ A. Reifenberger,⁶ C. Enss,⁶ M. Hempel,⁶ R. Klingeler,⁶ and S.-L. Drechsler^{1,§}

¹Leibniz Institute for Solid State and Materials Research, IFW-Dresden, D-01171 Dresden, Germany

²Institut für Theoretische Physik, TU Dresden, D-01062 Dresden, Germany

³Max-Planck Institute for Chemical Physics of Solids, D-01187 Dresden, Germany

⁴Institut für Festkörperphysik, TU Dresden, D-01062 Dresden, Germany

⁵Dresden High Magnetic Field Laboratory, Helmholtz-Zentrum Dresden-Rossendorf, 01314 Dresden, Germany

⁶Kirchhoff-Institute for Physics, University of Heidelberg, D-69120 Heidelberg, Germany

(Received 7 February 2013; revised manuscript received 23 April 2013; published 28 May 2013)

From the measurement and analysis of the specific heat of high-quality $K_{1-x}Na_xFe_2As_2$ single crystals we establish the presence of large T^2 contributions with coefficients $\alpha_{sc} \approx 30$ mJ/mol K³ at low T for both $x = 0$ and $x = 0.1$. Together with the observed \sqrt{B} behavior of the specific heat in the superconducting state both findings give evidence of d -wave superconductivity on almost all Fermi-surface sheets with an average gap amplitude of Δ_0 in the range of 0.4–0.8 meV. The derived Δ_0 and observed T_c agree well with the values calculated within Eliashberg theory, adopting a spin-fluctuation mediated pairing in the intermediate coupling regime.

DOI: 10.1103/PhysRevB.87.180507

PACS number(s): 74.25.Bt, 74.25.Dw, 74.25.Jb

In spite of the substantial experimental and theoretical research efforts to elucidate the symmetry and magnitude of the superconducting order parameter for the Fe pnictides,^{1,2} important questions concerning the doping evolution of the superconducting gap remain unsolved.^{3,4} In the stoichiometric parent compounds, nesting usually occurs between electron (el) and hole (h) Fermi-surface sheets (FSSs) and is responsible for the presence of long-range spin density wave (SDW) order. Superconductivity (SC) emerges when the SDW order is suppressed by doping or external pressure.² An s_{\pm} gap symmetry (nodeless gap function with opposite signs of the order parameters for el and h pockets) is believed to be realized in underdoped and optimally doped compounds, since the antiferromagnetic spin fluctuations (SFs) on the vector $Q = (\pi, \pi)$ connecting the el and h pockets remain strong in the vicinity of the SDW phase. The situation in the overdoped regime is not so clear. With further doping, el (h) bands disappear. Therefore, the paradigm of the *SF glue* at the vector $Q = (\pi, \pi)$ does not work. However, SFs have been found at some incommensurate propagation vectors.⁵ This has led to several proposals for the order parameters in heavily doped compounds: extended s , d , $s + id$ waves.^{3,6–8} Thus, even from a theoretical perspective the situation is still controversial.

One of the most interesting families from this point of view is $Ba_{1-x}K_xFe_2As_2$. Superconductivity in this compound occurs at $x \approx 0.15$.⁹ T_c increases with K doping up to $T_c \approx 38$ K for $x = 0.4$ (optimally doped regime). In this region experiments such as angle-resolved photoemission spectroscopy (ARPES)¹⁰ and thermal conductivity¹¹ show the absence of nodes in the gap, confirming an s -wave character of the order parameter. The evolution of the SC order parameter at high hole-doping levels is not well studied, so far. The measurements on polycrystalline samples show that T_c monotonically decreases with doping, reaching $T_c = 3.5$ K for KFe_2As_2 (K122).⁹ Whereas the el pockets are completely gone in K122, it was theoretically proposed that a change of

the order-parameter symmetry to d , s_{\pm} wave with accidental nodes, or $s + id$ should occur.^{3,6–8}

Until now, there is no consensus in the interpretation of available experimental data in favor of one of the proposed order parameters. Indeed, measurements of thermal conductivity^{12,13} and of the London penetration depth¹⁴ have been interpreted in terms of d -wave SC with line nodes on each FSS. In contrast, recent ultrahigh-resolution laser ARPES data for K122 have been interpreted in terms of a rather specific partial nodal s -wave SC having an unusual gap with “octet line-nodes” on the middle FSS, an almost-zero gap on the outer FSS, and a nodeless gap on the inner FSS.¹⁵ The specific-heat (SH) data for K122 above 0.4 K, only, were interpreted within a weak-coupling BCS-like multiple SC gap scenario with line nodes,^{16,17} adopting multiband, d -wave, or s -wave nodal SC. But at the same time an extremely strong coupling and/or correlated regimes with heavy quasiparticles were suggested for the normal state. Moreover, the authors of a subsequent SH study in magnetic fields¹⁸ doubted such an interpretation and denied the presence of a smaller second gap based on the observation of a nonintrinsic magnetic transition at low T , probably due to unknown magnetic impurities. Naturally, under such circumstances a T^2 and/or a \sqrt{B} behavior, generic for line nodes in the SC gap,^{19–21} could not be observed. Hence, further studies are necessary to clarify the symmetry of the SC order parameter and the magnitude of the coupling strength. These two issues are the main points of the present Rapid Communication.

$K_{1-x}Na_xFe_2As_2$ single crystals with $x = 0$ [K122] and $x = 0.1$ [(K,Na)122] were grown using KAs as a flux. SH data in various fields were obtained by a relaxation technique in a Physical Properties Measurement System (PPMS, Quantum Design). The magnetic ac susceptibility as a function of temperature was also measured by use of the PPMS. The T dependence of the electrical resistivity was measured using a standard four-probe dc technique. Two single crystals, K122 and

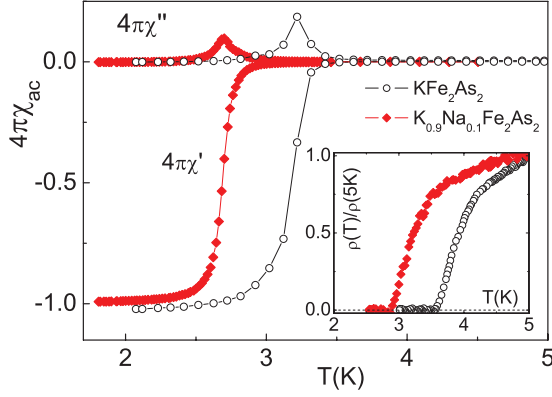


FIG. 1. (Color online) Temperature dependence of the complex volume ac susceptibility $\chi_{ac} = \chi' + i\chi''$ measured with an amplitude of 5 Oe and a frequency of $\nu = 1$ kHz. Inset: the normalized in-plane resistivity ρ measured in zero field.

(K,Na)122, were selected for SH measurements below 0.4 K using the heat-pulse technique within a dilution refrigerator.

The T dependence of the volume ac susceptibilities (χ' and χ'') of K122 and (K,Na)122 are shown in Fig. 1. The sharp transition with $4\pi\chi' \sim 1$ confirms the bulk nature of superconductivity and the high quality of our crystals. The T dependence of the in-plane electrical resistivity evidences a drop to zero at 3.6 K for K122 and at 2.9 K for (K,Na)122 in agreement with the diamagnetic onset seen in the χ_{ac} data. The resistivity ratio $RR = \rho(300K)/\rho(5K)$ is found to be ≈ 120 for (K,Na)122 with $\rho(5K) \approx 3.82 \mu\Omega$ cm which is smaller than $RR \approx 380$ for K122 with $\rho(5K) \approx 1.44 \mu\Omega$ cm. Therefore, the reduced T_c of (K,Na)122 can be attributed to pair-breaking effects due to the disorder induced by the Na doping.

The zero-field specific heat C of K122 and (K,Na)122 between 0.1 and 10 K is shown in Fig. 2. A clear sharp SC anomaly is observed at $T_c \approx 2.75$ K for (K,Na)122 and at $T_c \approx 3.5$ K for K122, in line with the resistivity and ac susceptibility data. The jump height of C at T_c is found to be $\Delta C/T_c \approx 40$ mJ/mol K² for (K,Na)122. This value is a bit reduced from ≈ 46 mJ/mol K² for K122. A zoom into the low- T range is shown in the inset of Fig. 2. We observe a

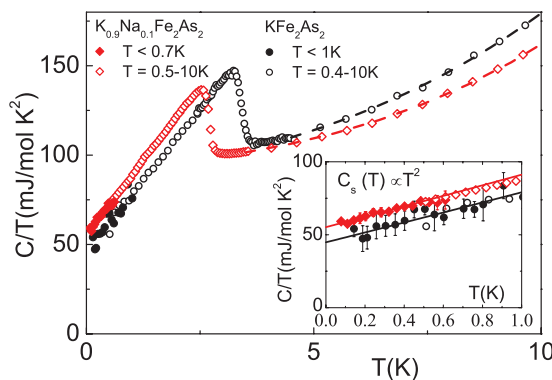


FIG. 2. (Color online) Specific heat C plotted as C/T vs T . Dashed lines: fits in the normal state (see text). Inset: zoom into the low- T region; solid lines: fits using Eq. (3). The data for K122 above 0.4 K are taken from Ref. 23.

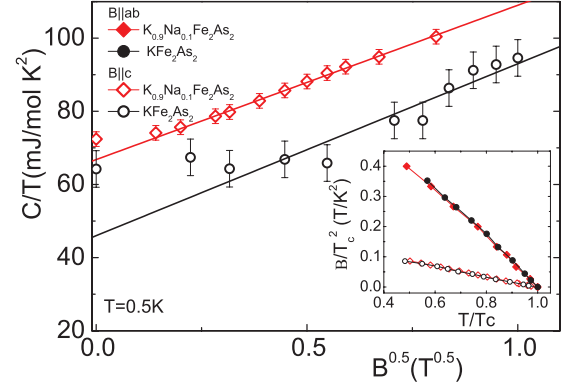


FIG. 3. (Color online) Field dependence of the specific heat, C/T , at 0.5 K. Solid lines: linear fits to define P_{sc} [see Eq. (4)]. Inset: the scaled upper critical fields for KFe_2As_2 ²³ and $K_{0.9}Na_{0.1}Fe_2As_2$ vs T/T_c .

pronounced T^2 behavior in the SH for both crystals. Notice that *no* kinks and/or small hump anomalies, predicted for the low- T region by weakly coupled two-band approaches,^{16,17} have been observed in our measurements. The field dependence of C/T at $T = 0.5$ K obtained from SH measurements in magnetic fields²² are shown in Fig. 3. The observed \sqrt{B} dependence together with the T^2 behavior provides direct evidence for a d -wave SC order parameter of $K_{1-x}Na_xFe_2As_2$, at least for $x \leq 0.1$.

The T dependence of the SH in the SC state allows one to determine whether the gap function possesses nodes. For instance, the exponential vanishing of C as in conventional s -wave SC is caused by the finite gap in the quasiparticle spectrum. In contrast, in the case of gap nodes, quasiparticles are generated to the largest extent in the vicinity of the gap nodes. In the case of line nodes, the quasiparticle excitation spectrum takes the form $E_k = \hbar\sqrt{v_F^2 k_\perp^2 + v_\Delta^2 k_\parallel^2}$,^{25,26} where k_\perp and k_\parallel are wave vectors perpendicular and parallel to the FSSs, respectively, v_F is the *renormalized* in-plane Fermi velocity at the position of the node, while $v_\Delta \approx \partial\Delta/\hbar\partial k$ is the slope of the gap at the node associated with the dispersion of the quasiparticles along the FS. This leads to a density of states (DOS) linear in energy. For the two-dimensional (2D) case it reads

$$N_{SC}(E) = \sum_i \frac{E}{\pi\hbar^2 v_F^i v_\Delta^i}, \quad (1)$$

where i denotes the sum over all nodes. Here, we would like to note that both materials considered are highly anisotropic, justifying the 2D approximation. The ratio of H_{c2} (in-plane vs out-of plane) according to the Fig. 3 inset suggests a large mass ratio $\Gamma^2 \approx 25$. This value agrees with density functional theory predictions for the ratio of the corresponding squared plasma frequencies.²³

Equation (1) results in a quadratic power-law dependence $C_s \propto \alpha_{sc} T^2$, with

$$\alpha_{sc}(\text{mJ/mol K}^3) \approx 0.283 \frac{\gamma_{el}(\text{mJ/mol K}^2)}{\Delta_0(\text{meV})} \quad (2)$$

taken from Refs. 19, 20, and 26 and valid for SC if both the impurity scattering rate and magnetic field scales are smaller than the temperature. Therefore, the observed T^2 behavior

suggests that this condition is fulfilled for both crystals studied. Using Eq. (1) we also assumed that the energy gap at $T = 0$, Δ_0 , is equal for all bands, while γ_{el} is a *renormalized* normal-state Sommerfeld coefficient, which is an average value over all FSSs (see the Supplemental Material²² for details). In this context, \varkappa is a dimensionless factor taking into account the anisotropy of $1/v_F$ at the position of the nodes with respect to the averaged isotropic value. According to our preliminary *ab initio* calculations for the k dependence of the DOS near the Fermi energy in the nodal direction, and the expected amount of the anisotropic mass renormalization due to anisotropic SF, $\varkappa \sim 1.1$ to 1.15. This range of values arises from the dominant contribution of the two inner FSSs around the Γ point in the Brillouin zone, which is somewhat reduced by a different antinodal anisotropy of the third FSS. The DOS of these three FSSs is about 90% of the total DOS. The resulting anisotropy is also in accord with the slightly larger gap value obtained in our Eliashberg-theory-based calculations (see below) than the value derived from Eq. (2).

To analyze the low- T SH data we use the ansatz

$$C = \gamma_r T + \alpha T^2 + \beta_3 T^3, \quad (3)$$

where the cubic term β_3 comes from phonons and is defined from the data in the normal state. The remaining terms stem from a magnetic cluster-glass contribution reported previously in Ref. 24 and from electronic degrees of freedom, which is the focus here. The best fit using Eq. (3) at $T \leq 0.4$ K yields $\gamma_r = 44.8$ mJ/mol K² and $\alpha = 33.7$ mJ/mol K³ for K122 and $\gamma_r = 55.2$ mJ/mol K² and $\alpha = 35.4$ mJ/mol K³ for (K,Na)122. It has been shown in Ref. 24 that the residual ‘‘Sommerfeld’’ coefficient γ_r of K122 mainly stems from a cluster-glass phase. At variance with K122, for (K,Na)122 an additional contribution to γ_r , exceeding 10 mJ/mol K², is caused by a disorder-induced pair-breaking effect¹⁹ in accord with the enhanced residual resistivity of this crystal. However, we emphasize that the T^2 contribution measured by α is not an extrinsic glassy contribution but stems from the generic electronic contribution in the superconducting state, only. The estimated contribution of the cluster glass amounts to $\alpha_{CG} \approx 2$ mJ/mol K³ for K122 and $\alpha_{CG} \approx 0$ for (K,Na)122.^{22,24} Hence, we argue that our observed large T^2 terms come mainly from quasiparticle excitations near line nodes. The resulting coefficients are $\alpha_{sc} \approx 32(3)$ mJ/mol K³ for K122 and $\alpha_{sc} \approx 35(1)$ mJ/mol K³ for (K,Na)122. Such a large T^2 contribution to the low T SH provides evidence of the d -wave character of the gap function.

In the case of a d -wave SC order parameter, $C(B)/T = P_{sc}\sqrt{B} + C(0)/T$ holds, if the energy associated with the Doppler shift $E_H = \hbar v_F(\pi B/\Phi_0)^{0.5}$ is large as compared to the thermal energy $E_T = k_B T$,²⁶ where Φ_0 is the flux quantum and $v_F = 4 \times 10^6$ cm/s.²³ According to our data shown in Fig. 3 for $T = 0.5$ K the field dependence of C/T follows a \sqrt{B} law at $B \gtrsim 0.06$ T which corresponds to $E_H/E_T \gtrsim 3$ in accord with the theoretical prediction.²⁶ Using the expressions (66) and (67) in Ref. 26 for P_{sc} and α_{sc} we get

$$\frac{P_{sc}}{\alpha_{sc}} \approx \frac{\pi^{5/2} \hbar M_1 v_F}{54 \zeta(3) k_B \Phi_0^{0.5}} \approx 1.8 M_1 (\text{K}/\text{T}^{0.5}), \quad (4)$$

where $M_1 \approx 1$ for a liquid vortex state and $M_1 = 1/\pi^{0.5} \approx 0.56$ for a completely disordered distribution.²⁶ This gives P_{sc} in the range of 30–60 mJ/mol K²T^{0.5} in accord with the experimental values ≈ 48 mJ/mol K²T^{0.5} for K122 and ≈ 42 mJ/mol K²T^{0.5} for (K,Na)122.

Now, we will check whether the value of α_{sc} can be satisfactorily described by the standard d -wave mechanism on all FSSs. Our analysis is based on Eq. (2), which was obtained within a BCS-like theory. But it works very well also in the case of strongly coupled cuprates.²⁷ Therefore, we expect its validity for pnictides, too. In addition, we analyze the relevant coupling constants with the help of the strong-coupling Eliashberg equations. The coupling constants λ_{sf} of the el-SF and λ_{ph} of the electron-phonon interaction together with the two bosonic spectral densities $\alpha^2 F(\omega)$ determine the gap value and T_c as well. A broad spectral density for intraband SF as obtained by recent inelastic neutron scattering measurements⁵ can be described as

$$\alpha^2 F(\omega) = \frac{\lambda_{sf} \Gamma_{sf}}{\pi} \frac{\omega}{\omega^2 + \Gamma_{sf}^2}, \quad (5)$$

where $\Gamma_{sf} = 7.9$ meV. For the phonons we assume a sharp Lorentzian spectral density with a width of 0.5 meV centered at $\omega_{ph} \sim 20$ meV. Notice that in our simple isotropic effective single-band model considered here for a d -wave superconducting order parameter, the el-ph coupling (EPC) drops out from the gap equation by symmetry and it enters only the equation for the Z function which describes the bosonic mass renormalization of the h -like quasiparticles.²² Thus, here the EPC results in a slight *suppression* of T_c and Δ_0 in contrast to the s_{\pm} case, where the superconductivity becomes stronger taking into account an intraband EPC. The SC gap and T_c calculated within Eliashberg theory and their dependence on the SF coupling constant λ_{sf} for $\lambda_{ph} = 0$ for the sake of simplicity and also for the more realistic case, with a weak el-ph coupling constant $\lambda_{ph} \sim 0.2$ (according to density functional theory based calculations²³) included, are shown in Fig. S2 of Ref. 22. To reproduce T_c , $\lambda_{\phi, sf} \sim 0.64 = 0.8 \lambda_{z, sf}$ should be adopted for K122, where the former describes the strength of the pairing interaction and the latter stands for the mass renormalization. (In the isotropic s -wave case $\lambda_{\phi, sf} = \lambda_{z, sf}$ holds.) These values for the coupling constants together with the calculated EPC constant $\lambda_{ph} \approx 0.2$ (Ref. 23) yield a total coupling constant of $\lambda_{z, tot} \approx 1$. As a result we get $\Delta_0^{\text{ET}} \approx 0.75$ meV, which is close to that in BCS theory $\Delta_0^{\text{BCS}} \sim 0.65$ meV obtained from the $2\Delta_0/T_c$ ratio for a d -wave superconductor in the 2D case:

$$\frac{2\Delta_0^{\text{BCS}}}{k_B T_c} = \frac{4\pi}{\gamma_E \sqrt{e}} \approx 4.28, \quad (6)$$

where γ_E is the Euler constant $\gamma_E = 1.781$. The obtained $\lambda_{z, tot}$ values suggest that we are in the regime of intermediate coupling and we may apply Eq. (2) to extract Δ_0 . Considering the isotropic case ($\varkappa = 1$) of Eq. (2), the same gap function for all bands and using the experimental electronic linear coefficient $\gamma_{el} = 52\text{--}68$ mJ/mol K²,²⁴ we estimate Δ_0^{expt} in the range of 0.4–0.7 meV, which is close to the values obtained above theoretically. It is also close to the larger gap values $\Delta_1 \approx 0.7\text{--}0.8$ meV obtained within effective weak-coupling

two-band models for the electronically weakly connected bands.^{16,17} However, the eight times smaller second gap Δ_2 (Refs. 16 and 17) with a comparable partial DOS for the second effective band would produce too large α_{sc} values exceeding our experimental value by a factor of 3 or more. Hence, such a multiband scenario can be excluded on the basis of our study.²⁸ In this context, we note that the SH jump $\Delta C/T_c\gamma_{el} \approx 0.7-0.9$ is close to the theoretical weak coupling value of 0.95 for a d -wave superconductor.²⁰ Thus, the proposed effective single-band d -wave scenario is in good agreement with experimental SH data.

Now, we compare the experimental value of α_{sc} with that for the “octet line nodes” scenario proposed in Ref. 15. In this case, the SH exhibits a T^2 behavior at low T , too; however, as shown in Ref. 22, the experimental value of α_{sc} is too large to be described by a single gap with octet line nodes on the middle (ζ) FSS only, as suggested in Ref. 15. Thus, we argue that the recently proposed interpocket s_{\pm} scenario⁸ with accidental line nodes on a particular FSS, only, is rather unlikely to be realized in the bulk as probed by the SH. Therefore, despite the multiband topology of $K_{1-x}Na_xFe_2As_2$, according to our SH data it behaves more or less like a single-band d -wave SC with corresponding line nodes on all FSSs as suggested by Reid *et al.* based on a thermal-conductivity study and universal scaling arguments valid for a single-band d -wave SC.^{11,12} It was predicted even before by theoretical calculations based on microscopic weak-coupling theory.³ However, quantitatively, in the interpretation of the thermal conductivity in Refs. 11 and 12 the nominal Sommerfeld coefficient γ_n was used and a possible magnetic contribution was not subtracted.

In summary, high-quality $K_{1-x}Na_xFe_2As_2$ ($x = 0,0.1$) single crystals were studied by specific heat. The large T^2 contributions and the \sqrt{B} behavior at low T provide evidence for the presence of line nodes in the superconducting gap. From the experimental data, an effective gap amplitude $\Delta_0^{expt} \sim 0.4-0.7$ meV was estimated. This Δ_0^{expt} and T_c agree well with the gap value calculated within Eliashberg theory for a one-band d -wave superconductor implying a moderately strong electron-boson coupling constant $\lambda_{z,tot} \approx 1$. This suggests that almost all, i.e., at least the three large Fermi-surface sheets with about 90% of the total DOS (according to the LDA) have comparable gap amplitudes. Our data provide quantitative evidence for the rather rare case of d -wave superconductivity in a Fe-pnictide system. A detailed comparison with the cuprates might be helpful to deepen our understanding of the pairing mechanism in both unconventional and still challenging superconducting families.

We thank D. Evtushinsky and V. Zabolotnyy for fruitful discussions as well as M. Deutschmann, S. Müller-Litvanyi, R. Müller, J. Werner, S. Pichl, K. Leger, and S. Gass for technical support. This work was supported by the DFG through SPP 1458 and the E.-Noether Program [WU 595/3-1 (S.W.)], and the EU-Japan Project (No. 283204 SUPER-IRON). I.M. and M.R. thank funding from RFBR (12-03-01143-a, 12-03-91674-ERA-a, 12-03-31717 mol-a), and S.J. from FOM (The Netherlands), and S.W. thanks the BMBF for support in the frame of the ERA.Net RUS project.

*M.A. and V.G. have equally contributed to the present paper.

[†]Present address: Lomonosov Moscow State University, GSP-1, Leninskie Gory, Moscow, 119991, Russian Federation.

[‡]Present address: Dept. of Physics and Astronomy, University of British Columbia, Vancouver, British Columbia, Canada V6T 1Z1.

[§]s.l.drechsler@ifw-dresden.de

¹P. J. Hirschfeld *et al.*, *Rep. Prog. Phys.* **74**, 124508 (2011).

²G. R. Stewart, *Rev. Mod. Phys.* **83**, 1589 (2011).

³R. Thomale, C. Platt, W. Hanke, J. Hu, and B. A. Bernevig, *Phys. Rev. Lett.* **107**, 117001 (2011).

⁴S. Maiti, M. M. Korshunov, T. A. Maier, P. J. Hirschfeld, and A. V. Chubukov, *Phys. Rev. Lett.* **107**, 147002 (2011).

⁵C. H. Lee *et al.*, *Phys. Rev. Lett.* **106**, 067003 (2011).

⁶A. Chubukov, *Ann. Rev. Cond. Mat. Phys.* **3**, 57 (2012).

⁷K. Suzuki, H. Usui, and K. Kuroki, *Phys. Rev. B* **84**, 144514 (2011).

⁸S. Maiti, M. M. Korshunov, and A. V. Chubukov, *Phys. Rev. B* **85**, 014511 (2012).

⁹S. Avci *et al.*, *Phys. Rev. B* **85**, 184507 (2012).

¹⁰D. V. Evtushinsky *et al.*, *Phys. Rev. B* **79**, 054517 (2009).

¹¹J. Ph. Reid *et al.*, *Supercond. Sci. Technol.* **25**, 084013 (2012).

¹²J. Ph. Reid *et al.*, *Phys. Rev. Lett.* **109**, 087001 (2012).

¹³J. K. Dong, S. Y. Zhou, T. Y. Guan, H. Zhang, Y. F. Dai, X. Qiu, X. F. Wang, Y. He, X. H. Chen, and S. Y. Li, *Phys. Rev. Lett.* **104**, 087005 (2010).

¹⁴K. Hashimoto *et al.*, *Phys. Rev. B* **82**, 014526 (2010).

¹⁵K. Okazaki *et al.*, *Science* **337**, 1314 (2012).

¹⁶H. Fukazawa *et al.*, *J. Phys. Soc. Jpn.* **80**, SA118 (2011).

¹⁷H. Fukazawa *et al.*, *J. Phys. Soc. Jpn.* **78**, 083712 (2009).

¹⁸J. S. Kim, E. G. Kim, G. R. Stewart, X. H. Chen, and X. F. Wang, *Phys. Rev. B* **83**, 172502 (2011).

¹⁹C. Kübert and P. J. Hirschfeld, *Solid State Commun.* **105**, 459 (1998).

²⁰B. Dóra and A. Virosztek, *Eur. Phys. J. B* **22**, 167 (2001).

²¹M. Sigrist and K. Ueda, *Rev. Mod. Phys.* **63**, 239 (1991).

²²See Supplemental Material at <http://link.aps.org/supplemental/10.1103/PhysRevB.87.180507> for details.

²³M. Abdel-Hafiez *et al.*, *Phys. Rev. B* **85**, 134533 (2012).

²⁴V. Grinenko *et al.*, *Phys. Status Solidi B* **250**, 593 (2013).

²⁵A. C. Durst and P. A. Lee, *Phys. Rev. B* **62**, 1270 (2000).

²⁶I. Vekhter, P. J. Hirschfeld, and E. J. Nicol, *Phys. Rev. B* **64**, 064513 (2001).

²⁷M. Ido *et al.*, *Physica C* **263**, 255 (1996).

²⁸In our opinion, the larger gap Δ_1 in a simple two-gap fit with $\Delta_1 \gg \Delta_2$ applied to the relatively “high- T ” SH data^{16,17} simulates the strong coupling effect included explicitly in our approach.